



New Hydrazine Derivatives as Corrosion for mild steel in phosphoric acid medium. Part B: Theoretical investigation.

M.E. Belghiti¹, Y. Karzazi^{1,2}, S. Tighadouini¹, A. Dafali^{*1},
C. Jama³, I. Warad⁴, B. Hammouti¹, S. Radi¹

¹Laboratory of Applied Chemistry and Environment (URAC-18), Faculty of Sciences, University of Mohammed Premier, B.P. 4808, 60046 Oujda, Morocco.

²National School of Engineering and Applied Sciences (ENSA), University of Mohammed Premier, B.P. 3, 32003 Sidi Bouaifj, Al Hoceima, Morocco.

³UMET-PSI, CNRS UMR 8207, ENSCL, Université Lille I, CS 90108, Villeneuve d'Ascq Cedex, F-59652, France

⁴Department of Chemistry, Science College. AN-Najah National University, P. O. Box 7, Nablus, State of Palestine

Received 15 Jan 2016, Revised 12 Feb 2016, Accepted 15 Feb 2016

* E-mail: dafali2@yahoo.fr

Abstract

Three hydrazine derivatives namely: 1,2-bis(pyrrol-2-ylidenemethyl)hydrazine (HZ1); 1,2-bis(thiophen-2-ylidenemethyl)hydrazine (HZ2); 1,2-Bis(furyl-2-ylidenemethyl)hydrazine (HZ3) were investigated as corrosion inhibitors of mild steel in Phosphoric acid using experimental and theoretical methods. In this part, Quantum chemical calculations based on DFT and QSAR methods were performed to determine the relationship between the molecular structure of hydrazines and their inhibition efficiencies. The quantum chemical parameters such as the localization of frontier molecular orbitals, E_{HOMO} , E_{LUMO} , energy gap(ΔE), dipole moment(μ), hardness(η), softness(S), the fractions of electrons transmit(ΔN), electrophilicity index (χ) and total energy charge were calculated and used to explicate the electron transfer mechanism between the inhibitor molecules and the steel surface. Furthermore, statistical equations were proposed using the multiple-linear and the nonlinear regression analysis.

Keywords: Hydrazine Derivatives, Corrosion, Mild Steel, Phosphoric Acid, DFT, QSAR.

1. Introduction

The corrosion is of fundamental, academic and industrial concern that has been subject of study of many corrosion scientists. The use of corrosion inhibitor is one of the most effective measures for protecting the metal surface against corrosion in acid environments [1]. A number of N-heterocyclic compounds in the aromatic or long carbon chain system have been reported as being effective inhibitors [2-3]. The remarkable inhibitory effect is reinforced by the presence of heteroatoms such as sulfur (S), oxygen (O) and nitrogen (N) in the ring which facilitates its adsorption on the metal surface following the sequence: -S- >=N->-O-> [4-5].

Researchers conclude that the adsorption on the metal surface depends mainly on the physicochemical properties of the inhibitor group, such as the functional group, electron density at donor site and π orbital character [6-14].

Density Functional theory (DFT) has been recently used [15-18], to describe the interaction between the inhibitor molecule and the surface as well as the properties of these inhibitors concerning their reactivity. This method is based on Beck's three parameter exchange functional and Lee-Yang-

Parr nonlocal correlation functional (B3LYP) [19-21] and the 6-311++G(2d,2p) orbital basis sets for all atoms as implemented in Gaussian 09 program. The molecular band gap was computed as the first vertical electronic excitation energy from the ground state using the time-dependent density functional theory (TD-DFT) approach as implemented in Gaussian 03 [22].

The aim of this paper is to study the relationships between the molecular structures of three hydrazine derivatives namely: 1,2-bis(pyrrol-2-ylidenemethyl)hydrazine (HZ1); 1,2-bis(thiophen-2-ylidenemethyl)hydrazine (HZ2) and 1,2-Bis(furyl-2-ylidenemethyl) hydrazine (HZ3) and their inhibition efficiencies obtained in part A [23]. Through the method of quantum chemical calculations, the structural parameters, such as the frontier molecular orbitals (MO) energy (E_{HOMO} and E_{LUMO}), energy gap (ΔE), dipole moment (μ), hardness (η), softness (σ), the fractions of electrons transfer from inhibitors to metal surface (ΔN), electrophilicity index (χ) and total energy charge were calculated and correlated to corrosion inhibition efficiencies using Quantitative structure and activity relationship (QSAR). The molecular structures for the investigated inhibitors are shown in Figure 1.

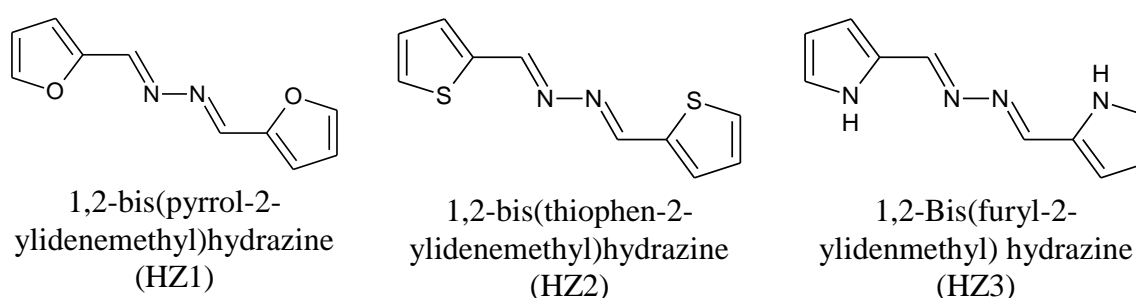


Figure 1: The Molecular structures of hydrazine derivatives HZ1, HZ2 and HZ3.

2. Theory and computational details

The frontier orbital HOMO and LUMO of a chemical species are very important in defining its reactivity. A good correlation has been found between the speeds of corrosion and E_{HOMO} that is often associated with the electron donating ability of the molecule. Survey of literature shows that the adsorption of the inhibitor on the metal surface can occur on the basis of donor-acceptor interactions between the π -electrons of the heterocyclic compound and the vacant d-orbital of the metal surface atoms [24], high value of E_{HOMO} of the molecules shows its tendency to donate electrons to appropriate acceptor molecules with low energy empty molecular orbitals. Increasing values of E_{HOMO} facilitate adsorption and therefore enhance the inhibition efficiency, by influencing the transport process through the adsorbed layer. Similar relations were found between the rates of corrosion and ΔE_{gap} ($\Delta E_{gap} = E_{LUMO} - E_{HOMO}$) [25-27]. The energy of the lowest unoccupied molecular orbital indicates the ability of the molecule to accept electrons. The lower the value of E_{LUMO} , the more probable the molecule would accept electrons. Consequently, concerning the value of the energy gap ΔE , larger values of the energy difference will provide low reactivity to a chemical species. Lower values of the ΔE will render good inhibition efficiency, because the energy required to remove an electron from the lowest occupied orbital will be low [28]. Another method to correlate inhibition efficiency with parameters of molecular structure is to calculate the fraction of electrons transferred from inhibitor to metal surface. According to Koopman's theorem [29], E_{HOMO} and E_{LUMO} of the inhibitor molecule are related to the ionization potential (I) and the electron affinity (A), respectively.

The ionization potential and the electron affinity are defined as $I = -E_{HOMO}$ and $A = -E_{LUMO}$, respectively. Then absolute electronegativity (χ) and global hardness (η) of the inhibitor molecule are approximated as follows [30]:

$$\chi = \frac{I + A}{2} \quad (1)$$

$$\eta = \frac{I - A}{2} \quad (2)$$

As hardness (η), softness (σ) is a global chemical descriptor measuring the molecular stability and reactivity and is given by:

$$\sigma = \frac{1}{\eta} \quad (3)$$

The chemical hardness fundamentally signifies the resistance towards the deformation or polarization of the electron cloud of the atoms, ions or molecules under small perturbation of chemical reaction. A hard molecule has a large energy gap and a soft molecule has a small energy gap [31].

The global electrophilicity (ω) index was introduced by Parr [32] as a measure of energy lowering due to maximal electron flow between donor and acceptor and is given by:

$$\omega = \frac{\mu^2}{2} \times \sigma \quad (4)$$

According to the definition, this index measures the propensity of chemical species to accept electrons. A good, more reactive, nucleophilic is characterized by lower value of μ , ω ; and conversely a good electrophilic is characterized by a high value of μ , ω . This new reactivity index measures the stabilization in energy when the system acquires an additional electronic charge ΔN from the environment. Thus the fraction of electrons transferred from the inhibitor to metallic surface, ΔN , is given by [31,33-34]:

$$\Delta N = \frac{\chi_{Fe} - \chi_{inh}}{2(\chi_{Fe} + \chi_{inh})} \quad (5)$$

Where χ_{Fe} and χ_{inh} denote the absolute electronegativity of iron and inhibitor molecule, respectively; η_{Fe} and η_{inh} denote the absolute hardness of iron and the inhibitor molecule, respectively. Using a theoretical χ_{Fe} value of 7.0 eV/mol according to Pearson electronegativity scale and η_{Fe} value of 0 eV/mol [30], ΔN , is the fraction of electrons transferred from inhibitor to, the steel surface, was calculated. Values of ΔN showed inhibition effect result from electrons donation. According to the simple charge transfer model for donation and back donation of charges [35], when a molecule receives a certain amount of charge, ΔN^+ ; then:

$$\Delta E^+ = \mu^+ \Delta N^+ + \frac{1}{2} \eta (\Delta N^+)^2 \quad (6a)$$

While when a molecule donates a certain amount of charge, ΔN^- , then:

$$\Delta E^- = \mu^- \Delta N^- + \frac{1}{2} \eta (\Delta N^-)^2 \quad (6b)$$

If the total energy change is approximated by the sum of the contributions of Equation (6a) and Equation (6b), assuming that the amount of charge back-donation is equal to the amount of charge received, $\Delta N^+ + \Delta N^- = 0$ ($\Delta N^+ = -\Delta N^-$), then ;

$$\Delta E_T = \Delta E_{back-donation} = \Delta E_{b-d} = \Delta E^+ + \Delta E^- \quad (7)$$

We replace ΔE^+ and ΔE^- by their expression in equations (6a) and (6b), we obtain:

$$\Delta E_{b-d} = (\mu^+ - \mu^-) \Delta N^+ + \eta (\Delta N^+)^2 \quad (8)$$

The most favorable situation corresponds to the case when the total energy change, $\Delta E_T = \Delta E_{b-d}$, becomes a minimum with respect to ΔN^+ , which implies that:

$$\Delta N^+ = \frac{-(\mu^+ - \mu^-)}{2\eta}$$

and that:

$$\Delta E_{b-d} = \frac{-(\mu^+ - \mu^-)^2}{4\eta} = -\frac{\eta}{4} = \frac{1}{8}(E_{HOMO} - E_{LUMO}) \quad (9)$$

The ΔE_{b-d} expression implies that when $\eta > 0$, and $\Delta E_{b-d} < 0$, the charge transfer to a molecule, followed by a back-donation from the molecule, is energetically favoured. In this context, hence, it is possible to compare the stabilization among inhibiting molecules, since there will be an interaction with the same metal, then, it is expected that it will decrease as the hardness increases.

3. Results and discussion

3.1. Quantum chemical calculations

The inhibition of steel using hydrazine derivatives HZ1, HZ2 and HZ3 as corrosion inhibitors were investigated experimentally, the classification of these inhibitors according to its inhibition efficiency is: HZ2 > HZ3 > HZ1 (see part A [23]). The higher inhibition efficiency of HZ2 than HZ3 and HZ1 is probably due to high electronegativity of thiophen (-S-) than pyrrol (=N-) and furan (-O-) ($O < N < S$) in cyclic compound attached to hydrazine ($RC=N-N=CR$).

These results indicate that the adsorption on the metal surface through the sulfur (-S-) atom of HZ2 will be easier and stronger than that through the nitrogen (=N-) and oxygen (-O-) atom of HZ3 and HZ1 respectively. Indeed, the enhancement of the adsorption is directly related to the increase of the inhibition efficiencies of HZ2 with respect to HZ3 and HZ1.

The geometric and electronic structures of (HZ1)[1,2-bis(pyrrol-2-ylidenemethyl)hydrazine]; (HZ2)[1,2-bis(thiophen-2-ylidenemethyl)hydrazine] and (HZ3)[1,2-Bis(furyl-2-ylidenemethyl)hydrazine] in solvent phase were calculated by the optimization geometric are presented in Figure 2.

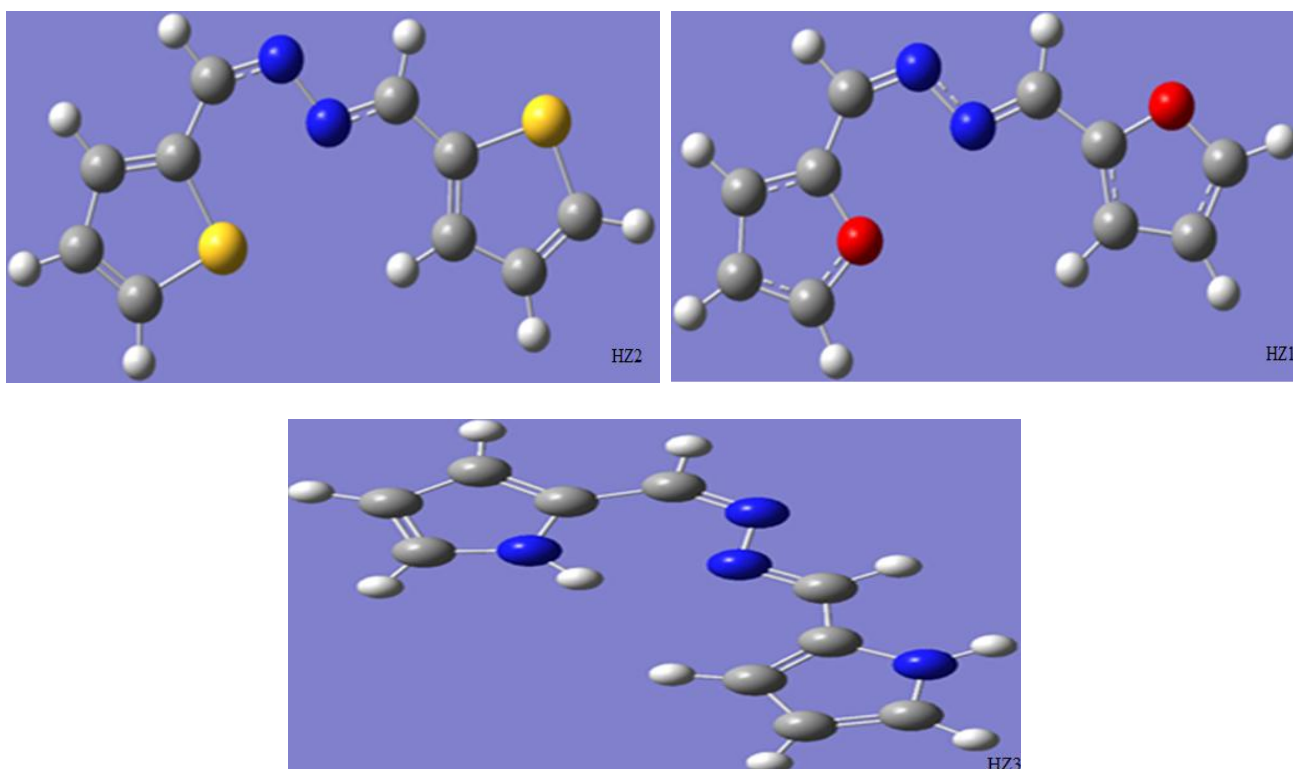


Figure 2: Optimized Structure of HZ1, HZ2 and HZ3 calculated in solvent phase with the DFT at the highest (B3LYP/6-311++G(2d,2p)) level.

Full geometry optimizations, [Figure 2](#), with no constraints of the three molecules under study were performed using DFT based on Beck's three parameter exchange functional and Lee–Yang–Parr nonlocal correlation functional (B3LYP) [19-20,36] and the 6-311++G(2d,2p) orbital basis sets for all atoms as implemented in Gaussian⁰⁹ program [21]. This approach has been proved to be a very powerful tool for studying corrosion inhibition mechanism [37-39].

The quantum chemical parameters for the neutral form of the inhibitors HZ1, HZ2 and HZ3 such as the energies of highest occupied molecular orbital (E_{HOMO}) and the lowest unoccupied molecular orbital (E_{LUMO}), the energy gap (ΔE_{gap}) between E_{HOMO} and E_{LUMO} , dipole moment(μ), ionization potential(I), electron affinity(A), absolute electronegativity(χ), global hardness(η), global electrophilicity index(ω), softness(σ), fraction of electrons transferred(ΔN) and back donation energy($\Delta E_{\text{b-d}}$) were calculated and gathered in [Table 1](#).

Table 1: Quantum chemical parameters for the neutral form of HZ1, HZ2 and HZ3 obtained in solvent phase with the DFT at the highest (B3LYP/6-311++G(2d,2p)) level.

Quantum chemical parameters	HZ3	HZ1	HZ2
E_{HOMO} (eV)	-5.582	-5.666	-5.636
E_{LUMO} (eV)	-1.5612	-1.322	-1.625
ΔE_{gap} (eV)	+4.021	+4.344	+4.019
I (eV)	+5.582	+5.666	+5.636
A (eV)	+1.5612	+1.322	+1.625
χ (eV)	+3.5716	+3.494	+3.630
η (eV)	+2.010	+2.172	+2.005
μ (Debye)	+2.2417	+1.8606	+2.5601
ω (eV)	+3.173	+2.810	+3.286
σ (eV) ⁻¹	+0.497	+0.460	+0.498
ΔN	+0.866	+0.807	+0.840
$\Delta E_{\text{b-d}}$ (eV) ⁻¹	-0.502	-0.543	-0.501
TE (eV)	-16321.22	-34820.79	-17420.87
IE (%)	84.93	79.50	85.57

According to the frontier molecular orbital theory (FMO) of chemical reactivity, transition of electron is due to interaction between highest occupied molecular orbital (HOMO) and lowest unoccupied molecular orbital (LUMO) of reacting species [40]. The energy of the highest occupied molecular orbital (E_{HOMO}) measures the tendency towards the donation of electron by a molecule. Therefore, higher values of E_{HOMO} indicate better tendency towards the donation of electron, enhancing the

adsorption of the inhibitor on mild steel and therefore better inhibition efficiency. E_{LUMO} indicates the ability of the molecule to accept electrons. The binding ability of the inhibitor to the metal surface increases with increasing of the HOMO and decreasing of the LUMO energy values. Frontier molecular orbital diagrams of HZ1, HZ2 and HZ3 are represented in Figure 3.

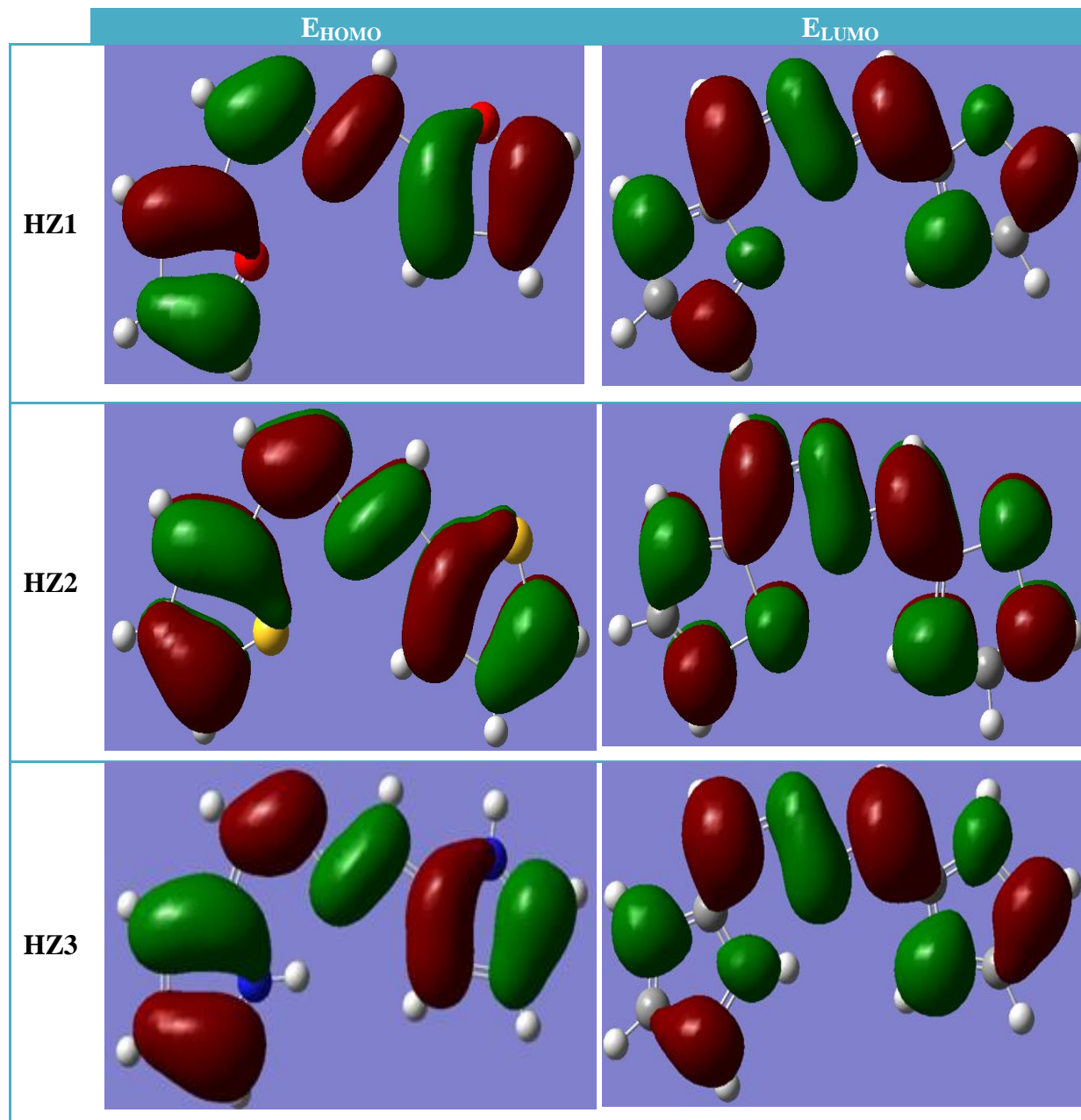


Figure 3: Schematic representation of HOMO and LUMO molecular orbitals of HZ1, HZ2 and HZ3 obtained in solvent phase with the DFT at B3LYP/6-311++G(2d,2p) level.

when we compared the three compounds HZ1, HZ2 and HZ3, the calculations show that the compound HZ2 has the highest HOMO level at -5.636eV and the lowest LUMO level at -1.625eV compared to the obtained parameters for HZ3 (-5.582 and -1.5612eV) and HZ1 (-5.666 and -1.322eV). This can explain that the highest inhibition efficiency of HZ2 is due to the increasing energy of the HOMO and the decreasing energy of the LUMO. This is the good agreement with the experimental observations suggesting that the inhibitor HZ2 has the highest inhibition efficiency than HZ3 and HZ1, respectively.

ΔE_{gap} is an important parameter as a function of reactivity of the inhibitor molecule towards the adsorption on metallic surface (physisorption and chemisorption). The results obtained show that the compound HZ2 has a lower ΔE_{gap} . This parameter provides a measure for the stability of the inhibitor molecule towards the adsorption on the metal surface. As ΔE_{gap} decreases, the reactivity of the molecule increases leading to increase the inhibition efficiency of the molecule. The value of ΔE_{gap} for HZ2, HZ3 and HZ1 are +4.019, +4.021 and +4.344eV, respectively. The results as indicated in Table 1 shows that inhibitor HZ2 has the lowest energy gap than HZ3 and HZ1 respectively, this means that the molecule could have better performance as corrosion inhibitor.

Absolute hardness (η), and Softness (σ), are important properties to measure the molecular stability and reactivity. It is apparent that the chemical hardness fundamentally signifies the resistance towards the deformation or polarization of the electron cloud of the atoms, ions or molecules under small perturbation of chemical reaction. A hard molecule has a large energy gap and a soft molecule has a small energy gap [41]. In our present study HZ2 with low hardness value +2.0055(eV) compared with other compound HZ1 and HZ3, respectively, have a low energy gap. Normally, the inhibitor with the least value of global hardness (hence the highest value of global softness) is expected to have the highest inhibition efficiency [42]. For the simplest transfer of electron, adsorption could occur at the part of the molecule where softness (σ), which is a local property, has a highest value [43]. With HZ2 the softness value of +0.498eV have the highest inhibition efficiency than (+0.497eV of HZ3 and 0.460eV of HZ1), respectively. This is also a good agreement with the experimental observations.

Dipole moment μ (Debye) is another important electronic parameter that results from non-uniformed distribution of charges on the various atoms in the molecule. The high value of dipole moment probably increases the adsorption between chemical compound and metal surface [44-45]. The energy of the deformability increases with the increase in μ , making the molecule easier to adsorb at the metal surface. The volume of the inhibitor molecules also increases with the increase of μ . This increases the contact area between the molecule and surface of metal and increasing the corrosion inhibition ability of inhibitors. In our study the value +2.5601(Debye) of HZ2 enumerates its better inhibition efficiency than HZ3 and HZ1, respectively.

The global electrophilicity index, ω , shows the ability of the inhibitor molecules to accept electrons. It is a measure of the stabilization in energy after a system accepts additional amount of electron charge ΔN from the environment [32]. In our case, the inhibitor HZ2 with high electrophilicity index value (+3.286eV) than the other compounds (+3.173eV of HZ3 and +2.810eV of HZ1), respectively, is the strongest nucleophilic and therefore has the highest inhibition efficiency [23].

The absolute electronegativity (χ) is the chemical property that describes the ability of a molecule to attract electrons towards itself in a covalent bond. According to Sanderson's electronegativity equalization principle [46], the molecule HZ2 with a high electronegativity quickly reaches equalization and hence low reactivity is expected which in turn indicates low inhibition efficiency. The Table 1 shows the order of electronegativity as HZ2>HZ3>HZ1. Hence an increase in the difference of electronegativity between the metal and inhibitor is observed in the order HZ2>HZ3>HZ1.

Calculated $\Delta E_{\text{b-d}}$ ($\Delta E_{\text{Back-donation}}$) values for the inhibitors as listed in Table 1 reveal that the order followed is: HZ2>HZ3>HZ1, which indicates that back-donation is favored for the molecule HZ2 which is the best inhibitor than HZ3 and HZ1, respectively. The results obtained by all this parameters are in good agreement with the experimental observations.

3.2. Mulliken atomic charges

The use of Mulliken population analysis to estimate the adsorption centers of inhibitors has been widely reported and it is mostly used for the calculation of the charge distribution over the whole skeleton of the molecule [47]. There is a general consensus by several authors that the more negatively charged heteroatom is, the more is its ability to adsorb on the metal surface through a donor-acceptor type reaction [33].

The Mulliken charge distributions of hydrazine derivatives compounds are calculated and presented in Table 2. The parameters were calculated for the heteroatoms only for simplicity.

Table 2 representing the effective atomic charges from Mulliken populations of HZ1, HZ2 and HZ3 inhibitors, shows that nitrogen (-N=) and oxygen (-O-) atoms carry more negative charges, while the remaining thiophen (-S-) atoms carry more positive charges. This means that the atoms carrying negative charges are the negative charge centers, which can offer electrons to the Fe atoms to form coordinate bond, and the atoms carrying positive charges are the positive charge centers, which can accept electrons from orbital of Fe atoms to form feedback bond.

Table 2: Calculated Mulliken atomic charges for heteroatom's of HZ1, HZ2 and HZ3 using DFT at the highest (B3LYP/6-311++G(2d,2p)) level.

Atoms	HZ2	HZ3	HZ1
S1	+0.317	*****	*****
S2	+0.268	*****	*****
N1	-0.292	-0.248	-0.291
N2	-0.301	-0.232	-0.299
O1	*****	*****	-0.425
O2	*****	*****	-0.449
N'1	*****	-0.447	*****
N'2	*****	-0.499	*****

This means that 1,2-bis(thiophen-2-ylidenemethyl)hydrazine(HZ2) has more excess charges than HZ3 and HZ1, respectively. This is due to the tautomeric effect between the hydrazine (-N=N-) and thiophen ring (Figure 4). This delocalization character of electrons yields to a more stable planar structure of HZ2. Thus, the optimized structure is in accordance with the fact that excellent corrosion inhibitors.

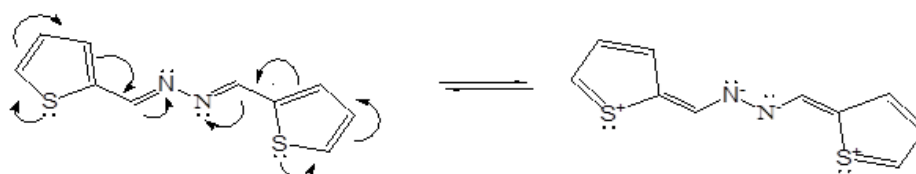


Figure 4: Schematic representation of the tautomeric forms of HZ2 molecule.

3.3. Quantitative structure and activity relationship (QSAR) consideration

QSAR was used to correlate the corrosion inhibition efficiency and molecular structures of the compounds under investigation. In attempt to correlate the quantum chemical parameters with the average experimental inhibition efficiencies showed that no simple relation or no direct trend relationship can be derived with the inhibition performance of these inhibitors. This is due to the complex interactions that are involved in the corrosion protection. Though a number of satisfactory correlations have been reported by other investigators [48-50] between the inhibition efficiency of various inhibitors used and some quantum chemical parameters, a composite index and a combination of more than one parameter [33,51] has been used to perform QSAR which might affect the inhibition efficiency of the studied molecules. Consequently, a relation may exist between the composite index and the average corrosion inhibition efficiency for a particular inhibitor molecule. Therefore, in the present study, mathematical models were tentatively fitted to the experimental values of the inhibition efficiency, IE_{cal} (%) as in equation (10) [52]. The objectives were:

- To obtain equations useful in predicting IE_{cal} (%) from the concentrations of the inhibitors and their quantum chemical parameters.
- To provide theoretical explanations for the effects of the different variables studied.

The first model investigated is an empirical linear model expressed as:

$$IE_{cal}(\%) = \beta_n X_n + \dots + \beta_3 X_3 + \beta_2 X_2 + \beta_1 X_1 + \beta_0 + \varepsilon \quad (10)$$

β_j : Constants obtained by regression analysis.

X_j : Independent variables consisting of quantum chemical values and the inhibitor concentration (C_j , μM).

ε : Error.

Where R^2 is the coefficient of determination, and SSE is the sum of squared errors defined as:

$$\sum (IE_{exp}(\%) - IE_{cal}(\%))^2 = SSE \quad (11)$$

The experimental results were fitted to the empirical model of equation (10) by forward multiple linear-regression with switching, using the software package NCSS¹⁰ [53-55]. The size of the selected subset of independent variables was limited to include only the variables that are significant at the 0.05 level.

The estimated equations when using the quantum chemical values of the molecules are:

$$IE_{cal}(\%) = (19.25)E_{HOMO} + (-51.26)E_{LUMO} + (4.355)C_j \quad (12)$$

$$R^2 = 0.9688 \quad SSE = 89.30$$

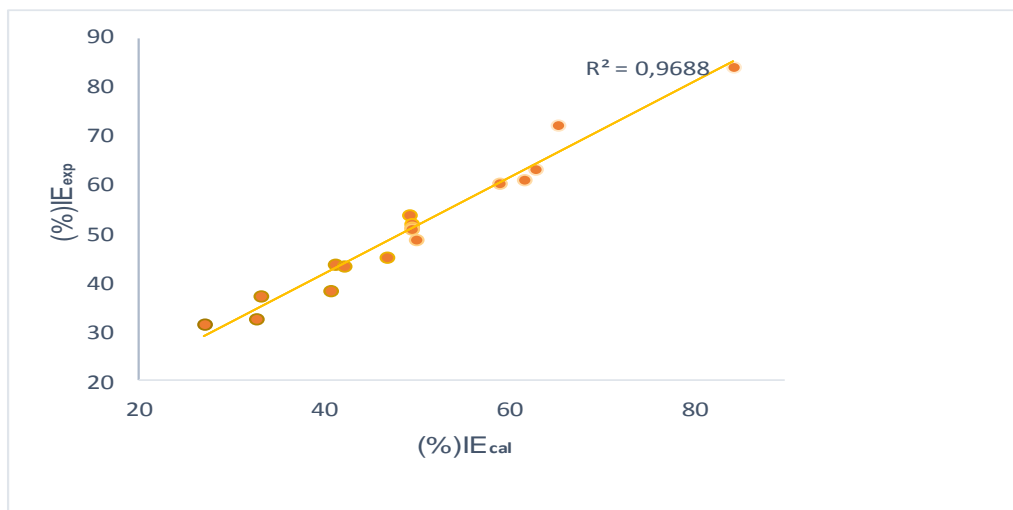


Figure 5: Correlation between experimental inhibition efficiency $IE_{exp}(\%)$ and calculated inhibition efficiency $IE_{cal}(\%)$ obtained from QSAR model from equation (12).

Equation (12) produce close estimate of $IE_{cal}(\%)$, the equation(10) is useful in predicting the inhibition efficiency. **Figure 5**, is a plot of the estimated versus the experimental $IE_{exp}(\%)$ values and it can be seen that the estimates are close to the experimental values. An inspection of the residual plots (not shown) did not suggest obvious deviation from homoscedasticity (constant variance).

Beside the linear model of Equation (10), there is also a nonlinear model that is commonly applied in corrosion inhibition studies. This non-linear model was first proposed by Lukovits et al. [34] for the

interaction of corrosion inhibitors with metal surface in phosphoric acid solutions. It has a theoretical derivation based on Langmuir adsorption isotherm, and is expressed as:

$$IE_{cal}(\%) = \frac{[AX_j + B]C_j \times 100}{1 + (AX_j + B)C_j} \quad (13)$$

A and B: Constants obtained by regression analysis.

X_j: Quantum chemical index (E_{HOMO}, E_{LUMO}, ΔE_{gap}, μ, etc.) characteristic for the molecule.

C_j: Inhibitor concentration in μM.

The estimated equations when using the quantum chemical values of the molecules are:

$$IE_{cal}(\%) = \frac{[0.0049\mu + 0.275\Delta E + 0.464E_{LUMO} - 2.807E_{HOMO} - 0.597]C_j \times 100}{1 + (0.0049\mu + 0.275\Delta E + 0.464E_{LUMO} - 2.807E_{HOMO} - 0.597)C_j} \quad (14)$$

R²= 0.7382 SSE= 226.4

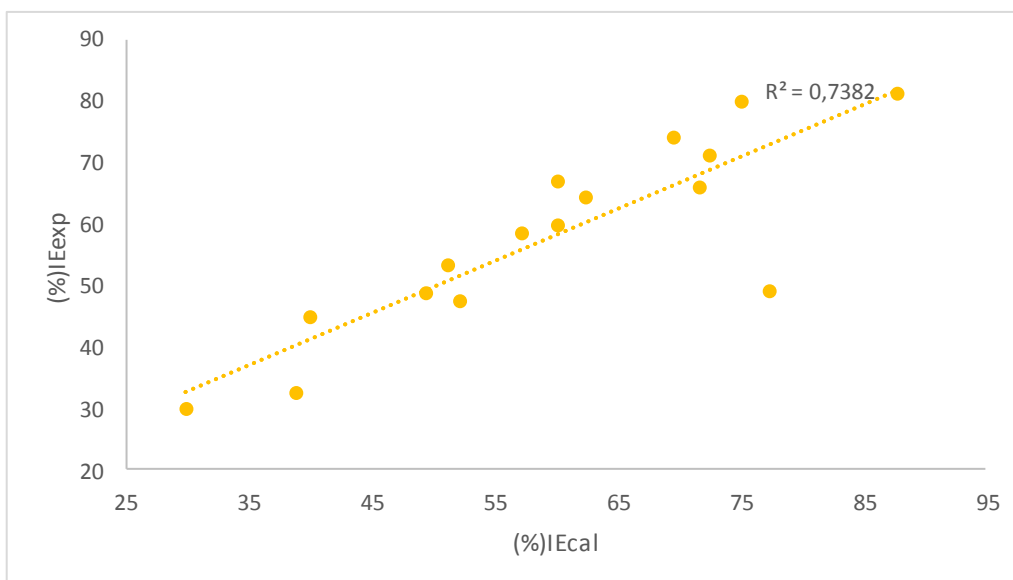


Figure 6: Correlation between experimental inhibition efficiency IE_{exp} (%) and calculated inhibition efficiency IE_{cal} (%) obtained from QSAR model from Equation (13).

Table 3 : Asymptotic correlation matrix of parameters estimated in Equation (13).

	C _i	ΔE	μ	E _{HOMO}	E _{LUMO}
C _i	+1.0000	-0.9995	-0.9994	+0.9993	+0.9996
ΔE	-0.9997	+1.0000	+0.9995	-0.9991	-0.9997
μ	-0.9995	+0.9998	+1.0000	-0.9992	-0.9995
E _{HOMO}	+0.9994	-0.9998	-0.9990	+1.0000	+0.9995
E _{LUMO}	+0.9997	-0.9993	-0.9990	+0.9996	+1.0000

An inspection of Figure 6 shows that Equation (14) estimated almost identical values of IE_{cal} (%). Table 3 is the asymptotic correlation matrix of parameters estimated in Equation (13), it is clear that the parameters are very highly correlated.

The multiple-linear regression analyses fitted the theoretical data well and the calculated inhibition efficiency of HZ1, HZ2 and HZ3, was found to be close to their experimental corrosion inhibition

efficiencies especially in the neutral form ($R^2 = 0.9401$). The results obtained in this study indicated that indeed, in acidic media, one should consider the neutral species involved because they seem to represent better the actual experimental situation. The QSAR approach is adequately sufficient to forecast the inhibitor efficiencies using the theoretical approach.

Conclusion

The following results can be drawn from this study:

- ✓ The relationships between inhibition efficiency of mild steel in phosphoric acid (2M) and the E_{HOMO} , E_{LUMO} , ΔE_{gap} and μ of the hydrazine derivatives compounds were calculated using the DFT at the highest (B3LYP/6-311++G(2d,2p)) level of theory using Gaussian09W program package. Quantum chemical calculations have shown that apart from HZ1, HZ2 and HZ3 adsorptions of the molecule are take place through S, N and O atoms. The locations containing N-heteroatoms with high electron density is the most possible sites for bonding the mild steel surface through electron donations to the metal surface.
- ✓ QSAR approach has been utilized in this study and a good relationship was found between the experimental results of the previous studies with that calculated in this work.
- ✓ The calculated inhibition efficiency was found to be close to the experimental inhibition with coefficient of correlation (R^2) of 0.9401.

References

1. Zhang Q. B., Hua Y. X., *Electrochim. Acta* 54 (2009) 1881.
2. Dafali A., Hammouti B., Touzani R., Kertit S., Ramdani A., Elkacemi K., *Anti-corros. Meth. & Mat.*, 49 (2002) 96.
3. Machnikova E., Whitmire K.H., Hackerman N., *Electrochim. Acta*, 53 (2008) 6024.
4. Dafali A., Hammouti B., Mokhlisse R., Kertit S., Elkacemi K., *Corros. Sci.*, 45 (2003) 1619.
5. Donnelly B., T.C. Downier T.C., Grzeskowiak R., Hamburg H.R., Short D., *Corros. Sci.*, 18 (1978) 109.
6. Singh A.K., Quraishi M.A., *Corros. Sci.*, 52 (2010)152.
7. Zarrouk A., Hammouti B., Dafali A., Bentiss F., *Ind. Eng. Chem. Res.*, 52 (2013) 2560.
8. De Souza F.S., Spinelli A., *Corros. Sci.*, 51(2009) 642.
9. Li X., Deng S., Fu H., Li T., *Electrochim. Acta* 54 (2009) 4089.
10. Dafali A., Hammouti B., Kertit S., *J. Electrochem. Soc. Ind.* 50 N°2 (2001) 62.
11. Popova A., Sokolova E., Christov M., *Corros. Sci.* 45 (2003) 33.
12. Benabdellah M., Touzani R., Aouniti, A., Dafali A., Elkadiri S., Hammouti B., Benkaddour M., *Phys. Chem. News*, 37 (2007) 63.
13. Rallas S., Gulerman N., Erdeniz H., *Farmaco* 57 (2002) 171.
14. Zarrouk A., Zarrok H., Salghi R., Hammouti B., Al-Deyab S.S., Touzani R., Bouachrine M., Warad I., Hadda T.B., *Int. J. Electrochem. Soc.* 7 (2012) 6353-6364.
15. Wang W., Li Z., Sun Q., Du A., Li Y., Wang J., Bi S., Li P., *Corros. Sci.* 61 (2012) 101.
16. Ma H., Chen S., Liu Z., Sun Y., *J. Mol. Struct. (THEOCHEM)* 774 (2006) 19.
17. Zarrouk A., Bouachrine M., Hammouti B., Dafali A., Zarrok H., *J. Saudi Chem. Soc.* 18 (2014) 550.
18. Musa A.Y., Mohamad A.B., Kadhum A.H., Takriff M.S., Ahmoda W., *J. Ind. Eng. Chem.* 18 (2012) 551.
19. Becke A. D., *J. Chem. Phys.* 98 (1993) 1372.
20. Lee C., Yang W., Parr R.G., *Phys. Rev. B.*37 (1988) 785.
21. Frisch M.J. et al., *Gaussian, Inc. Wallingford CT*, (2009).
22. Frisch M.J. et al., *GAUSSIAN 03, Revision B.03, Gaussian, Inc., Wallingford, CT, 2004.*

23. Belghiti M. E., Tighadouini S., Karzazi Y., Dafali A., Hammouti B., Radi S., Solmaz R. *J. Mater. Environ. Sci.* 7 (1) (2016) 337.
24. Li W., Zhao X., Liu F., Deng J., Hou B., *Mater. Corros.* 60 (2009) 287.
25. Hasanov R., Sadikoglu M., Bilgic S., *Appl. Surf. Sci.* 253 (2007) 3913.
26. Amin M.A., Khaled K.F., Fadl-Allah S.A., *Corros. Sci.* 52 (2010) 140.
27. Wang H., Wang X., Wang H., Wang L., Liu A., *J. Mol. Model.* 13 (2007) 147.
28. Obot I.B., Obi-Egbedi N.O., Umoren S.A., *Int. J. Electro Chem.Sci.* 4 (2009) 863.
29. Dewar M.J.S., Thiel W., *J. Am. Chem. Soc.* 99 (1977) 4899.
30. Pearson R.G., *Inorg. Chem.* 27 (1988) 734.
31. Sastri V.S., Perumareddi J.R., *Corrosion (NACE)* 53 (1997) 617.
32. Parr R.G., Szentpaly L., Liu S., *J. Am. Chem. Soc.* 121 (1999) 1922.
33. Obot I.B., Obi-Egbedi N.O., *Corros. Sci.* 52 (2010) 657.
34. Lukovits I., Kalman E., Zucchi F., *Corrosion (NACE)* 57 (2001) 3.
35. Gomez B., Likhanova N.V., Dominguez-Aguilar M.A., Vela R., Martinez-Palou A., Gasquez J., *J. Phys. Chem. B* 110 (2006) 8928.
36. Becke A.D., *J. Chem. Phys.* 96 (1992) 9489.
37. Zarrouk A., Hammouti B., Dafali A., Zarrok H., Touzani R., Bouachrine M., Zertoubi M., *Res. Chem. Intermed.* 38 (2012) 1079.
38. Bentiss F., Lebrini M., Lagrenee M., *Corros. Sci.* 47 (2005) 2915.
39. Karzazi Y., Belghiti M.E., Dafali A., Hammouti B., *J. Chem. Pharm. Res.* 6 (2014) 689.
40. Musa A.Y., Kadhun A.H., Mohamad A.B., Rohama A.A.B., Mesmari H., *J. Mol. Struct.* 969 (2010) 233.
41. Hasanov R., Sadikoglu M., Bilgic S., *Appl. Surf. Sci.* 253 (2007) 3913.
42. Ebenso E. E., Isabirye D. A., Eddy N.O., *Int. J. Mol. Sci.* 11(2010) 2473.
43. Li X., Deng S., Fu H., Li T., *Electrochim. Acta*, 54 (2009) 4089.
44. Quraishi M.A., Sardar R., *J. App. Electrochem*, 33(12) (2003) 1163.
45. Zarrouk A., Hammouti B., Dafali A., Bouachrine M., Zarrok H., Bouhkris S., Al-Deyab S.S., *J. Saudi Chem. Soc.*, 18 (2014) 450.
46. Geerlings P., DeProft F., *Int. J. Mol. Sci.* 3 (2002) 276.
47. Sahin M., Gece G., Karci E., Bilgic S., *J. Appl. Electrochem.* 38 (2008) 809.
48. Zhang S.G., Lei W., Xia M.Z., Wang F.Y., *J. Mol. Struct. THEOCHEM.* 732 (2005) 173.
49. Bentiss F., Lebrini M., Lagrenee M., Traisnel M., Elfarouk A., Vezin H., *Electrochim. Acta*, 52 (2007) 6865.
50. Eddy N.O., Ibok U.J., Ebenso E.E., El-Nemr A., El-Sayed, El-Ashry H., *J. Mol. Model*, 15 (2009) 1085.
51. Khaled K. F., Babic-Samradzija K., Hackerman N., *Electrochim. Acta*, 50 (2005) 2515.
52. El Ashry E. H., El Nemr A., Esawy S. A., Ragab S., *Electrochim. Acta*, 51 (2006) 3957.
53. Zo G. Y., *Stat. Methods Med. Res.*, 22(6) (2013) 630.
54. Bentiss F., Lagrenee M., *J. Mater. Environ. Sci.* 2 (2011) 13-17.
55. Messali M., Asiri M.A.M., *J. Mater. Environ. Sci.* 4 (2013) 770-785.

(2016) ; <http://www.jmaterenvirosci.com>